Mechanism of amyloid plaque formation suggests an intracellular basis of Aβ pathogenicity

Ralf P. Friedrich[a,1,3], Katharina Tepper[a,b,1], Raik Rönicke[c], Malle Soom[a], Martin Westermann[d], Klaus Reymann[c], Christoph Kaether[a], and Marcus Fändrich[a,b,e,2]

[a]Leibniz Institute for Age Research, Fritz Lipmann Institute, 07745 Jena, Germany [b]Max-Planck Research Unit for Enzymology of Protein Folding, 06120 Halle (Saale), Germany [d]Center of Electron Microscopy, Friedrich Schiller University, 07743 Jena, Germany [c]Leibniz Institute for Neurobiology (IfN), 39118 Magdeburg, Germany [e]Martin-Luther University Halle-Wittenberg, 06120 Halle (Saale), Germany

Edited by David S Eisenberg, University of California, Los Angeles, CA, and approved October 14, 2009 (received for review April 24, 2009)

The formation of extracellular amyloid plaques is a common pathobiochemical event underlying several debilitating human conditions, including Alzheimer's disease (AD). Considerable evidence implies that AD damage arises primarily from small oligomeric amyloid forms of Aβ peptide, but the precise mechanism of pathogenicity remains to be established. Using a cell culture system that reproducibly leads to the formation of Alzheimer's Aβ amyloid plaques, we show here that the formation of a single amyloid plaque represents a template-dependent process that critically involves the presence of endocytosis- or phagocytosis-competent cells. Internalized Aβ peptide becomes sorted to multivesicular bodies where fibrils grow out, thus penetrating the vesicular membrane. Upon plaque formation, cells undergo cell death and intracellular amyloid structures become released into the extracellular space. These data imply a mechanism where the pathogenic activity of Aβ is attributed, at least in part, to intracellular aggregates.

Alzheimer | aggregation | neurodegeneration | prion | protein misfolding

Amyloid fibrils are fibrillar polypeptide aggregates consisting of a cross-β structure (13–4). A vast number of natural or nonnatural polypeptide chains have been reported to from amyloid fibrils (1, 3). These fibrils relate structurally to the infectious prions from Creutzfeldt-Jakob disease (5). In Alzheimer's disease (AD), amyloid fibrils are formed from Aβ peptide (6). This peptide is produced at cholesterol-rich regions of neuronal membranes and secreted into the extracellular space (7). Aβ peptide can vary in length. The 40-residue peptide Aβ(1–40) represents the most abundant Aβ species in normal and AD brains, followed by the 42-residue peptide Aβ(1–42) (6). Aβ(1–40) and Aβ(1–42) are able to adopt many differently shaped aggregates including amyloid fibrils (8–11) as well as nonfibrillar aggregates that are sometimes termed also Aβ "oligomers" (12, 13). It is not well established which Aβ state is most responsible for AD or why. Nor exists consensus on the precise subcellular location of Aβ pathogenicity. Aβ peptide and Aβ amyloid plaques typically occur outside the cell (14, 15), but considerable evidence points towards a potential relevance of intracellular Aβ (16–20).

To shed some light on the mechanism of Aβ aggregation and pathogenicity we here report a cell-culture model that faithfully enables analysis of the formation of amyloid plaques inside the culture dish. We show that living cells are critical for plaque formation and that plaque biogenesis involves Aβ accumulation within intracellular vesicles, such as multivesicular bodies (MVBs). The fibrils formed by Aβ under these conditions impair the ordered vesicular functions by growing out and penetrating the vesicular membrane. Ultimately, these events lead to the death of the affected cells and the extracellular accumulation of previously intracellular amyloid structures.

Results

Different Types of Cells Can Promote Amyloid Plaque Formation. Previous analyses suggested an implication of living cells in amyloid plaque formation from Aβ peptide (21). To test this hypothesis, we examined different cell types for their potential plaque promoting activity. Analyzed cells include simian kidney cells (COS), human embryonic kidney-293 cells (HEK-293), human neuroblastoma cells (SH-SY5Y), laryngeal carcinoma cells (HEp-2), murine (J-774A.1), and human monocytic cells (THP-1). The latter were activated and differentiated into macrophages using phorbol 12-myristate 13-acetate. To induce plaque formation, freshly dissolved Aβ(1–40) peptide was added to the culture medium. Plaque formation was monitored either by using the filter retention assay (Fig. 1*A*) or Congo red (CR) green birefringence (Fig. 1*C–F* and Fig. S1). The filter retention assay separates Aβ plaques from soluble Aβ by retention on a filter membrane. Immunological detection of Aβ allows semiquantitative read outs. CR green birefringence is an anisotropic optical effect of CR-bound amyloid fibrils that can be visualized by polarizing microscopy. CR birefringence provides qualitative evidence for presence of amyloid-like cross-β structure. Filter retention shows plaque formation with all types of cells examined here (Fig. 1*A*). Qualitatively similar results are obtained with CR green birefringence. Representative images for THP-1 cells are shown in Fig. 1*C–F*. In addition, we noted that presence of minute amounts of preformed Aβ(1–40) fibrils presents a seeding effect. It accelerates plaque formation (Fig. S2*A*) and reduces the well-to-well variance.

Although different types of cells share a common ability to promote amyloid plaque formation, we note differences in the extent to which this reaction is supported by different cell lines. THP-1 and J-774A.1 cells show the strongest effects. These cell lines are highly endocytosis- or phagocytosis-competent and belong to the group of mononuclear phagocytes. Primary mononuclear phagocytes also enable Aβ plaque formation, as shown for murine microglia, murine macrophages, and human macrophages (Fig. S1). The lowest plaque yield is detected in cultures of SH-SY5Y neuroblastoma cells (Fig. 1*A*). Plaque formation can be reduced by addition of the known amyloid inhibitor CR (Fig. S2*B*) or by replacing wild type Aβ with the Aβ variant Val18-Pro (Fig. S2*C*) that possesses a low intrinsic aggregation propensity (22). Effectively no discernible plaque formation is seen in the absence of cells or in the presence of dead cell bodies after paraformaldehyde (PFA) or methanol fixation (Fig. 1*B*). Hence,

Author contributions: K.R., C.K., and M.F. designed research; R.F., K.T., R.R., M.S., and M.W. performed research; R.F., K.T., R.R., M.W., C.K., and M.F. analyzed data; R.F., K.T., C.K., and M.F. wrote the paper.

Conflict of interest statement: The authors declare no conflict of interest.

This article is a PNAS Direct Submission.

[1]Both authors contributed equally to this work.

[2]To whom correspondence should be addressed: Max-Planck Research Unit for Enzymology of Protein Folding and Martin-Luther University Halle-Wittenberg, Weinbergweg 22, 06120 Halle (Saale), Germany. E-mail: fandrich@enzyme-halle.mpg.de.

[3]Present address: Max Delbrueck Center for Molecular Medicine (MDC), 13125 Berlin, Germany.

This article contains supporting information online at www.pnas.org/cgi/content/full/0904532106/DCSupplemental.

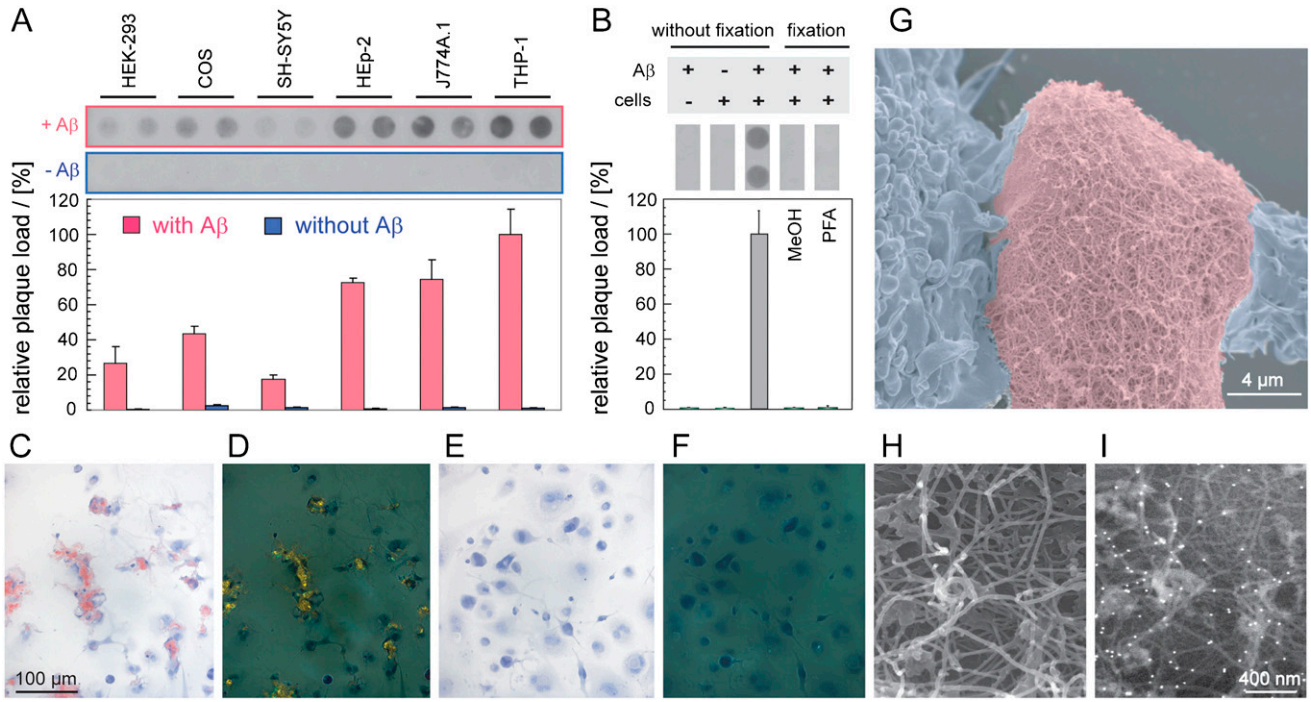

Fig. 1. Cell-dependent formation of Aβ amyloid plaques. (*A*) Amyloid load obtained with different cell lines after incubation for 3 days in the presence of freshly dissolved 60 µg/mL Aβ(1–40). On day zero, the medium was additionally supplemented with 100 ng/mL seeds, corresponding to 0.2% of the total amount of Aβ peptide added on day zero. Representative raw data images from filter retention assay and densitometric quantifications shown ($n = 30$; 0%: background; 100%: amyloid load with THP-1 cells). (*B*) Amyloid load in wells containing living THP-1 cells (without fixation), Aβ(1–40) or dead THP-1 cell bodies as indicated ($n = 12$). Dead THP-1 cell bodies were obtained by fixation of THP-1 cells using methanol (MeOH) or PFA. MeOH and PFA were removed before addition of Aβ(1–40) peptide or seeds. Medium supplements as in panel (*A*). (*C–F*) Congo red stained THP-1 cell culture after 4 d incubation with freshly dissolved Aβ(1–40) and seeds (*C*, *D*) or after 8 d incubation without any Aβ (*E*, *F*). Bright field (*C*, *E*) or dark field (*D*, *F*) polarizing microscopy images shown. (*G–I*) SEM image of an amyloid plaque from THP-1 cell culture after 6 d incubation, showing a fibrillar ultrastructure. Medium supplements as in panel (*A*). (*G*) Color coding: blue, cell bodies; red, amyloid plaque. (*H*, *I*) Secondary electron SEM image (*H*) or mixed secondary: backscatter electron SEM image (20:80 ratio) (*I*) of an Aβ immunogold labeled plaque. White points show immunogold labeled Aβ.

living cells are required for plaque biogenesis (Fig. 2*A*). This conclusion is further corroborated by time-lapse video microscopy (Fig. 2*B*) that does not provide evidence for any cell-independent plaque nucleation or growth events. Instead, plaque formation occurs always in close spatial association with cells or within the cell bodies.

Based on their biochemical, biophysical, and tinctorial properties, resultant Aβ assemblies represent bona fide amyloid plaques. They produce CR green birefringence (Fig. 1*C–F*). Aβ is retained by the filter retention assay (Fig. 1*A*). Scanning electron microscopy (SEM) shows the extracellular localization and fibrillar constitution of the plaques (Fig. 1*G*). Aβ immunogold labeling demonstrates that the fibrils are constructed from Aβ peptide (Fig. 1*H–I*). Plaques stain intensively with Alcian blue, consistent with the presence of glycosaminoglycans (Fig. S3). Light microscopy (Fig. 1*C*) and SEM (Fig. 1*G*) reveals an infiltration of the plaques by THP-1 cells. Altogether these properties correspond closely to known hallmark characteristics of amyloid plaques in natural tissue deposits (23).

Nucleation-Dependent Formation of Single Aβ Amyloid Plaques. Time-lapse video microscopy analysis of Aβ plaque formation is based on promofluor-488 labeled Aβ(1–40), termed here $^{488}A\beta$. $^{488}A\beta$ allows fluorescent visualization of plaque formation, whereas cellular changes were monitored with phase contrast microscopy (Fig. 2*B*). Quantification of the fluorescence intensity within the area of an emerging plaque demonstrates the presence of two well-resolved phases, termed lag phase and growth phase (Fig. 3). This type of kinetic behavior is highly characteristic for amyloid fibrillation reactions and indicates its nucleation-dependence (24). Although such biphasic growth profiles have been observed previously as bulk solution properties of whole samples or biological systems (Fig. S4*C*) (21, 24, 25), the present analysis demonstrates this type of kinetic behavior also at the level of a single amyloid plaque.

Analysis of time-lapse video microscopy images recorded during the lag phase shows only weak and dispersed fluorescence signals within the area of a prospective plaque (Fig. 2*B*, 33 h). Onset of the growth phase is marked by the appearance of a single spot of bright fluorescence intensity, the plaque nucleus (Fig. 2*B*, 40 h). This spot continuously increases in fluorescence intensity during the growth phase, implying that Aβ peptide is continuously incorporated into the plaque. There has been no evidence for an influx of discrete fluorescence foci into the emerging plaque; therefore, plaques do not grow by clumping together preformed plaque-like structures. However, there were single observations of two independently nucleated plaque nuclei that eventually coalesce into a single common plaque.

Individual plaques from the same sample can show profound differences in their formation kinetics. These variations are evident from the different length of the lag phase, termed lag time. The lag time can vary for the analyzed culture from 18 to 51 h (Fig. 3). A similar heterogeneity has been described previously for in vitro fibrillation reactions as well (24, 25), or molecular dynamics simulations (26). Such heterogeneity may arise from the stochastic nature of the nucleation reaction or from the formation of differently structured nuclei. Furthermore, the observed time frame of plaque growth resembles the time frame of Aβ plaque growth reported for transgenic AD mice (27).

Support for the template-dependence of plaque formation comes from observations that preformed fibrils seed plaque formation in our system. Addition of preformed Aβ(1–40) fibrils

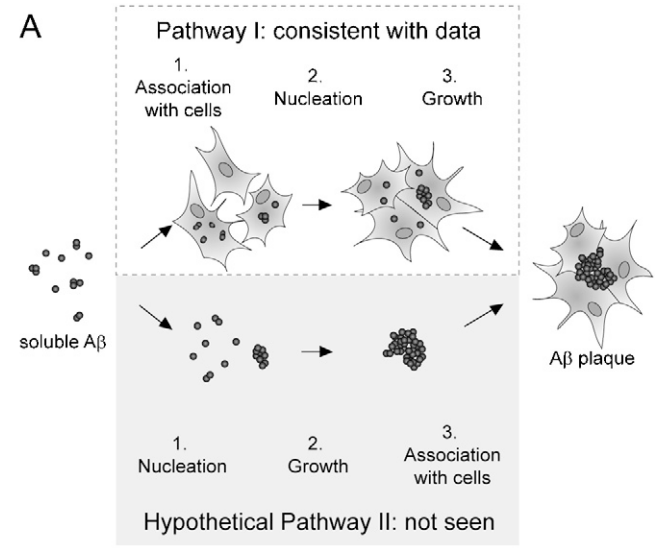

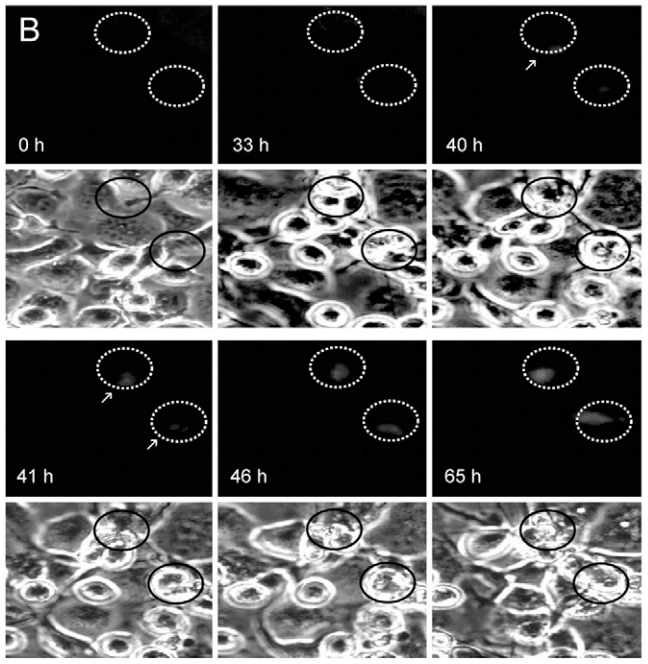

Fig. 2. Time-lapse video microscopy images of amyloid plaque formation. (*A*) Schematic representation of the mechanism of amyloid plaque. Hypothetical pathway (gray background) of amyloid plaque formation and pathway consistent with presented data (white background). (*B*) THP-1 cells were incubated with 60 μg/mL Aβ(1–40), containing 10% soluble ^{488}Aβ and monitored with fluorescence (*Top*) and phase contrast (*Bottom*) microscopy. Each well was supplemented 100 ng/mL seeds, corresponding to 0.2% of the total amount of Aβ peptide added on day zero. Beginning of amyloid plaque formation is indicated by arrows. Ellipses are drawn to guide the eye.

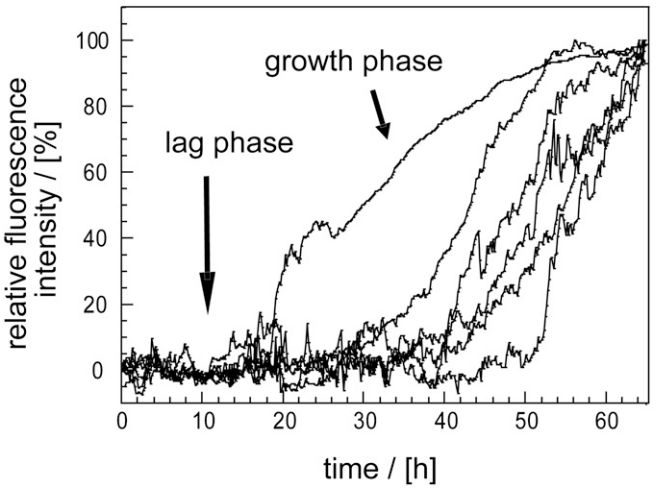

Fig. 3. Stochastic variability of single plaque formation. Quantification of the fluorescence signal of single amyloid plaques formed in THP-1 cell culture. The maximum fluorescence level was set to 100%.

seeds the formation of plaques (Fig. S4*A*). Control reactions without cells show no significant plaque formation (Fig. S4*B*). We have tested different amyloid fibrils that were prepared in vitro from different polypeptide chains with respect to their seeding efficiency. These fibrils were formed from Aβ(1–40) and Aβ(1–42), transthyretin, murine serum amyloid A (mSAA) protein, insulin, glucagon, apomyoglobin, and a peptide corresponding to the G-helix of myoglobin. Thus, the analyzed fibrils include polypeptide sequences responsible for amyloid disorders, such as transthyretin or mSAA, whereas other polypeptide sequences are only known to form amyloid in vitro, such as the G-helix (1, 28, 29). Measured seeding efficiencies are strictly template-dependent; hence, different fibrils differ considerably in their seeding efficiency (Fig. S4*A*). Aβ fibrils tend to seed more efficiently than non-Aβ fibrils. Furthermore, Aβ(1–40) fibrils produce stronger effects than Aβ(1–42) fibrils which is consistent with previous observations (30). The high seeding efficiency of Aβ-derived fibrils, consistent with concepts that emphasize the importance of sequential complementarity in amyloid formation (2).

As a next step we have tested the seeding efficiency of various fibrils using an in vitro assay, where Aβ(1–40) fibrillation is monitored with thioflavin-T (ThT) fluorescence (Fig. S4*C*). Analysis of lag times shows considerable variations for different seeds (Fig. S4*D*). A short lag time means efficient nucleation, whereas a long lag time means inefficient nucleation (25). The various seeds differ significantly in the efficiency by which they can promote the nucleation of Aβ(1–40) plaques in cell culture. The order of seeding activities seen within the in vitro fibrillation assay corresponds to the one observed in cell culture (Fig. S4*A*). The correlation coefficient *R* of the two datasets is 0.74 (Fig. S4*E*). We conclude that the seeding activity in THP-1 cell culture follows the intrinsic, biophysical propensity by which Aβ(1–40) peptide extends a given seed whereas cell-specific processes, such as differences in the processing or transport of the various seeds, are not required to explain the encountered differences.

Extracellular Aβ Plaques are Preceded by Intracellular Intermediates. In accord with our above observations that living cells are relevant for plaque formation, we find that impairment of cellular functions with cytochalasin B (Cyt) or latrunculin B (Lat) potently reduces the plaque yield (Fig. 4*A*). Control experiments show that the reduced plaque formation cannot be explained by a direct antiamyloidotic activity of the two agents or by their potential cytotoxicity. Cyt and Lat do not affect the fibril nucleation kinetics, as shown by an indistinguishable lag time with or without Cyt or Lat (Fig. 4*B*). They do not alter the fibril elongation kinetics, measurable from the growth rate (Fig. S5*A*), or the fibril yield, as determined from the pellet fraction after centrifugation (Fig. S5*B*). Furthermore, cell viability measurements carried out by using the lactate dehydrogenase assay do not show any discernible cytotoxic effect of the two agents (Fig. 4*C*). However, cell viability measurements carried out in the absence of Lat or Cyt show that the process of Aβ amyloid plaque formation itself is detrimental to THP-1 cells (Fig. 4*D*).

Given that Cyt and Lat are known inhibitors of endo- and phagocytosis reactions these data imply that plaque formation might

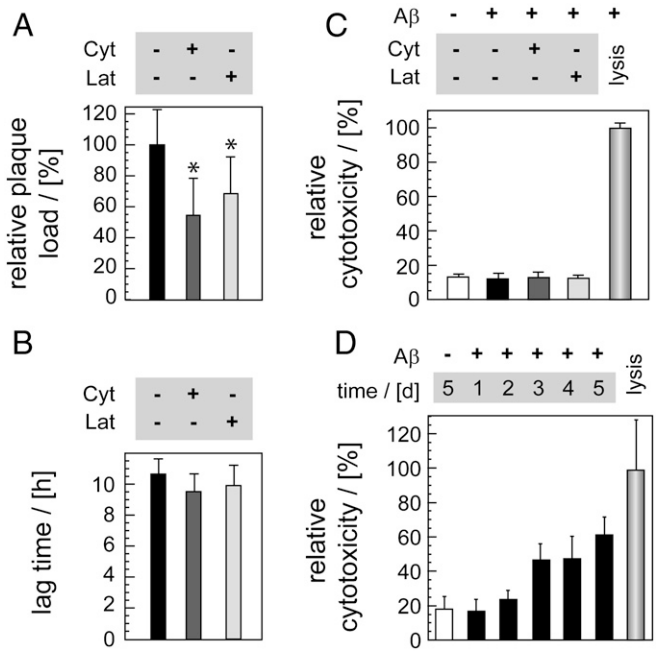

Fig. 4. Relevance of Aβ uptake for plaque formation. (*A*) Cytochalasin B (Cyt) or latrunculin B (Lat) decrease plaque formation in THP-1 cells as shown with the filter retention assay after 1 d incubation ($n = 24$). The value obtained with untreated THP-1 cells was set to 100%. Medium supplements as described in Fig. 1*A*. (*B*) Lag time of in vitro Aβ(1–40) fibrillation reactions with or without Lat or Cyt, monitored with ThT fluorescence ($n = 8$). (*C*, *D*) Cell viability measurements with the lactate dehydrogenase assay. (*C*) Cyt or Lat are not toxic to THP-1 cells (1 d incubation, no Aβ addition, $n = 7$). (*D*) Plaque formation reduces THP-1 cell viability (different time points shown, $n = 14$). The value obtained with full cell lysis was set to 100%. Panels (*A*–*C*) use always 6 μM Cyt or 2.5 μM Lat.

require, at least transiently, the internalization of Aβ peptide. Support for this notion comes from confocal-like fluorescence microscopy (CFM) and transmission electron microscopy (TEM). The two techniques consistently show intracellular Aβ peptide structures prior to plaque formation or cell death. CFM shows that Aβ uptake commences within 5 min after addition of the peptide to the culture medium (Fig. S6). Internalized Aβ occurs in the form of discrete and relatively small-sized fluorescent spots (Fig. S6), consistent with its intravesicular localization. A significant fraction of the internalized peptide shows colocalization with Alexa Fluor 555-conjugated transferrin (^{555}TF), a marker of clathrin-dependent endocytosis (Fig. S6). Hence, THP-1 cells internalize Aβ peptide partly through this pathway. THP-1 cells differ in this property from cultured neurons that show only very little, if any, Aβ uptake by clathrin-dependent endocytosis (31). Consistent with the relevance of Aβ internalization, SH-SY5Y neuroblastoma cells are found here to possess a relatively low plaque-promoting activity (Fig. 1*A*). Control experiments with compartment markers for Golgi apparatus (giantin) or endoplasmic reticulum (calnexin) do not show colocalization with ^{488}Aβ. CFM could not detect significant colocalization between internalized ^{488}Aβ and markers for early endosomes or lysosomes, including lysosomal-associated membrane protein 2, rhodamine-dextrane and Lyso Tracker (Figs. S6, S7). In addition, cell freeze fracturing coupled with Aβ immunogold labeling and TEM analysis was unable to observe substantial levels of Aβ within small unilaminar vesicles, such as endosomes or lysosomes. The low colocalization efficiency with lysosomal markers implies a low concentration of Aβ in this compartment. Possible explanations hereof include retention in other compartments or prelysosomal degradation.

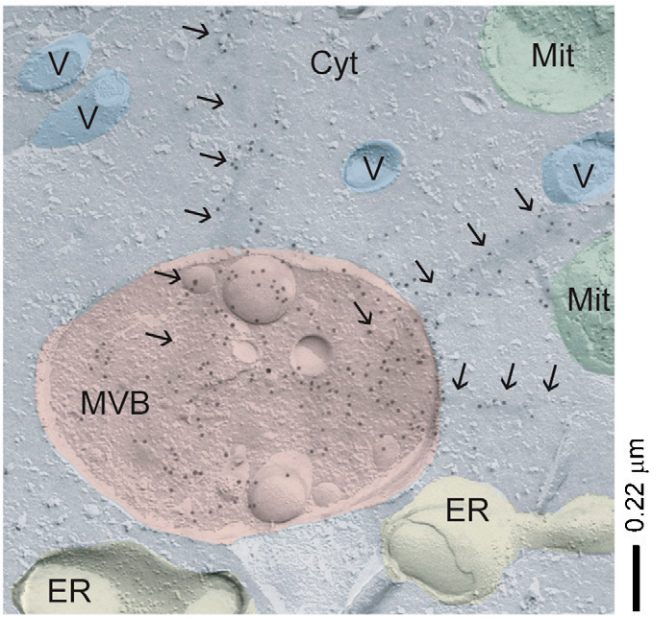

Fig. 5. Aβ-dependent perturbation of the MVBs. TEM images of freeze-fractured J774A.1 cells showing Aβ-positive staining (immunogold labels) within MVBs and membrane penetration through fibrillar Aβ bundles (arrows). Possible assignments of other vesicular structures (V), mitochondria (Mit), endoplasmic reticulum (ER) and cytoplasm (Cyt) shown.

Interestingly, TEM analysis reproducibly demonstrates Aβ within MVBs (Fig. 5, Fig. S8). MVBs represent multifunctional compartments that functionally interact with other vesicular pathways (32); and this central vesicular compartment appears to be primarily affected by the action of Aβ peptide. MVBs do not only engulf Aβ peptide within their lumen. Several TEM images show bundles of Aβ fibrils that penetrate the vesicular membrane and extend into the cytoplasm (Fig. 5, Fig. S8). In some cases there was also evidence for a deformation of the MVB shape, possibly arising from their stiff, fibrillar content (Fig. S8). These abnormalities are seen within cells that appear by all other morphological means intact and viable, indicating the encountered Aβ-induced disturbances of MVB function precede cell death.

Discussion

The presented data imply a mechanism for the formation of Aβ amyloid plaques in which initially soluble and extracellular Aβ peptide becomes internalized and sorted into MVBs. Upon spontaneous nucleation or in the presence of suitable fibril seeds, fibrils grow out, disturb the ordered MVB function and penetrate the vesicular membrane. Ultimately cells die and all intracellular structures, including all intracellular amyloid species, become released into the extracellular space.

This mechanism is consistent with substantial evidence from AD brain tissues and AD animal models. Specifically, it reconciles the known extracellular deposition of terminal amyloid plaques in AD patients or AD mouse models (15, 23) with numerous observations from AD patients (33), AD mouse models (34) and Aβ-transgenic *Drosophila melanogaster* flies (35) showing that Aβ species may also accumulate inside the cell, including MVBs (16, 36, 37), lysosomes or other vesicular compartments (38–40). The present observation of an intracellular route of amyloid plaque formation is consistent with observations that extracellular amyloid plaques typically contain a spectrum of proteins that are originally intracellular. For instance, AD plaques commonly contain lysosomal proteases or molecular chaperones

from the heat shock protein families Hsp70 or Hsp20 (17, 36, 41–43).

It is important to emphasize, however, that the cell death seen in our cell-culture system represents the cell death associated with plaque biogenesis. This cell death needs not be the same as the one responsible for the massive neuronal loss in AD patients. Neuronal loss has been shown not to correlate well with plaque formation in AD patients (44) and also AD mouse models can present tremendous plaque loads despite very little neuronal death (45). A possible explanation for these in vivo observations is provided by our present data showing that different types of cells are evidently able to promote plaque formation (Fig. 1*A*).

Although the cells responsible for in vivo plaque formation remain to be established, we show here that different types of cells possess the general ability to promote this reaction. Hence, amyloid plaque formation in vivo needs not to depend on or affect primarily the neuronal cells. Out of all tested cells we find that SH-SY5Y human neuroblastoma cells yield the lowest plaque levels (Fig. 1*A*). Previous analyses of human AD samples or animals imply the involvement of various types of cells, including neurons (46), astrocytes (47), smooth muscle cells (48), microglia or other mononuclear phagocytes (49, 50).

The role of mononuclear phagocytes remains particularly controversial. Although these cells seem important for amyloid plaque biogenesis in some extracerebral amyloidoses (51–53), their net physiological role in AD may rather be plaque clearance (54). Here, we use these cells because of their relatively high plaque-promoting activity. Nevertheless, we suggest that, despite the relatively general ability of cells to promote plaque formation, in vivo plaque formation may well involve only some cell types. However, their involvement will depend rather on other specific cellular properties such as migration behavior or endocytotic activity along with the precise and tissue-dependent conditions of Aβ exposure such as local Aβ concentrations or effective exposure times.

Regarding the role of Aβ internalization it is possible to explain the need of these reactions for plaque biogenesis with several observations. For instance, internalization increases the local Aβ concentration and restricts the peptide within a confined space. This situation is known to favor intermolecular aggregation reactions of amyloid fibril formation (55, 56). In addition, internalization exposes Aβ peptide to factors that are known to promote its fibrillation, such as the ganglioside GM1 (57). And indeed, GM1 has been reported to occur of the inside of several vesicular membranes (58).

Support for the notion that Aβ-internalization by nonneuronal cells represents a possible pathway toward Aβ aggregation comes also from observations that neuronal expression of Aβ in transgenic animals produces intravesicular Aβ aggregates within neighboring glia cells (59). Evidently, these glia cells must have internalized the Aβ peptide that was secreted initially from adjacent neuronal cells.

The current data are also relevant in the context of previous proposals suggesting that cytoplasmatic Aβ is key to Aβ pathogenicity (19). However, it has remained largely unclear how Aβ peptide, which occurs typically within extracellular compartments may transit into the cytoplasm. Using immunogold labeling combined with cell freeze-fracturing and EM we here show the penetration of MVB membranes and the translocation of a certain proportion of Aβ peptide into the cytoplasm (Fig. 5, Fig. S8). Therefore, our observations provide a direct link between the normal localization of Aβ peptide within extracellular space or vesicular compartments and a translocation into the cytoplasm in the course of cell death. Moreover, there has been previous evidence that the loss of the integrity of endosomal/lysosomal membranes represents an early event of Aβ pathogenesis (60) and it was suggested that the leakage of intracellular vesicles may lead to Aβ-dependent cell death (60). Further work will be required to ascertain whether or not these pathways are responsible for the encountered cell death in our model system as well. As pointed out above there may be more than one route of Aβ to pathogenicity and the precise processes responsible for the neuronal loss of AD patients remain to be established. Several studies have suggested an implication of nonfibrillar Aβ aggregates, sometimes termed oligomers.

The present characterization of different types of cells, all able to promote the formation of Aβ plaques in cell-culture, provides a solid basis for designing further experiments that scrutinize the mechanism of AD plaque formation in cell culture or within native brain tissues. A better understanding of these steps will also pave the way for targeting the earliest steps of plaque formation with conformation-specific antibodies (13, 61) or with small molecules that redirect aggregation pathways into a more favorable direction (62).

Materials and Methods

Th-T Aggregation Kinetics Measurements. Unless indicated otherwise, samples contained 50 μM Aβ(1–40) in 100 μL, 50 mM Hepes buffer, pH 7.4, 20 μM ThT, 10 mM sodium azide with or without 0.1 μg seeds. Instrumental settings were used as described (63).

Amyloid Plaque Formation in Cell Culture. Plaque formation was induced by supplementing the culture medium with freshly dissolved Aβ(1–40) peptide (final concentration in the well: 60 μg/mL). Immediately before Aβ was added to the medium, lyophilized, recombinant Aβ(1–40) peptide was dissolved at 10 mg/mL concentration in double-distilled water, sonicated for 2 min, followed by centrifugation for 15 min (10, 500 × g). Freshly dissolved Aβ was replenished each time the culture medium was replaced. In some experiments the medium was additionally supplemented with seeds (see *SI Text* for details on cell culture and sample seeding).

Light Microscopy. Time-lapse fluorescence and phase contrast images were recorded at 10 min intervals with a CCD-camera (Axiocam MRm, Zeiss). Data analysis was performed with Zeiss software (AxioVs40 V4.5). Confocal (Zeiss LSM510) and confocal-like (Zeiss Axiovert 200 Apotome) fluorescence microscopy were recorded with cells that were either immuno-stained or exposed to fluorescent particles (see *SI Text* for details).

Electron Microscopy. Scanning electron microscopy was performed at a FE-SEM, LEO 1530 Gemini instrument whereas transmission images were viewed with an EM902A transmission electron microscope (Zeiss). For freeze-fracture replica immunogold labeling samples were fractured and replicated in a BAF400T (BAL-TEC) freeze-fracture unit at −150 °C using a double-replica stage. The replica immunogold labeling was performed using an Aβ(1–16) antibody diluted 1:25 and a 1:50 diluted second goat antimouse antibody coupled with 10 nm gold (British Biocell International). Other sample work up details are described in *SI Text*.

Statistical Analysis. Errors or error bars represent the standard deviation. Significance (*) was established with an unpaired t-test up to a level of $p = 0.05$.

ACKNOWLEDGMENTS. We thank A. Kleyman, J.P. Tuckermann, M. Strassburger, and K. Wieligmann for technical advice and J. Kelly for the generous gift of transthyretin protein. The work of M.F. is supported by grants from Bundesministerium für Bildung und Forschung (BioFuture) and Deutsche Forschungsgemeinschaft (SFB 610). M.F. and K.R. acknowledge additional funding through the Exzellenznetzwerk Biowissenschaften (Land Sachsen-Anhalt).

1. Chiti F, Dobson CM (2006) Protein misfolding, functional amyloid, and human disease. *Annu Rev Biochem*, 75:333–366.
2. Sawaya MR, et al. (2007) Atomic structures of amyloid cross-beta spines reveal varied steric zippers. *Nature*, 447(7143):453–457.
3. Fändrich M (2007) On the structural definition of amyloid fibrils and other polypeptide aggregates. *Cell Mol Life Sci*, 64(16):2066–2078.
4. Cohen FE, Kelly JW (2003) Therapeutic approaches to protein-misfolding diseases. *Nature*, 426(6968):905–909.

5. Prusiner SB (1998) Prions. *Proc Natl Acad Sci USA*, 95(23):13363–13383.
6. Finder VH, Glockshuber R (2007) Amyloid-beta aggregation. *Neurodegener Dis*, 4(1):13–27.
7. Simons M, et al. (1998) Cholesterol depletion inhibits the generation of beta-amyloid in hippocampal neurons. *Proc Natl Acad Sci USA*, 95(11):6460–6464.
8. Meinhardt J, Sachse C, Hortschansky P, Grigorieff N, Fändrich M (2009) Abeta(1–40) fibril polymorphism implies diverse interaction patterns in amyloid fibrils. *J Mol Biol*, 386(3):869–877.
9. Lührs T, et al. (2005) 3D structure of Alzheimer's amyloid-beta(1–42) fibrils. *Proc Natl Acad Sci USA*, 102(48):17342–17347.
10. Kodali R, Wetzel R (2007) Polymorphism in the intermediates and products of amyloid assembly. *Curr Opin Struct Biol*, 17(1):48–57.
11. Sachse C, Fändrich M, Grigorieff N (2008) Paired beta-sheet structure of an Abeta (1–40) amyloid fibril revealed by electron microscopy. *Proc Natl Acad Sci USA*, 105 (21):7462–7466.
12. Haass C, Selkoe DJ (2007) Soluble protein oligomers in neurodegeneration: Lssons from the Alzheimer's amyloid beta-peptide. *Nat Rev Mol Cell Biol*, 8(2):101–112.
13. Glabe CG (2008) Structural classification of toxic amyloid oligomers. *J Biol Chem*, 283 (44):29639–29643.
14. Pepys MB (2006) Amyloidosis. *Annu Rev Med*, 57:223–241.
15. Meyer-Luehmann M, et al. (2003) Extracellular amyloid formation and associated pathology in neural grafts. *Nat Neurosci*, 6(4):370–377.
16. Takahashi RH, et al. (2002) Intraneuronal Alzheimer Aeta42 accumulates in multivesicular bodies and is associated with synaptic pathology. *Am J Pathol*, 161(5): 1869–1879.
17. Rajendran L, et al. (2007) Increased Abeta production leads to intracellular accumulation of Abeta in flotillin-1-positive endosomes. *Neurodegener Dis*, 4(2–3):164–170.
18. Oakley H, et al. (2006) Intraneuronal beta-amyloid aggregates, neurodegeneration, and neuron loss in transgenic mice with five familial Alzheimer's disease mutations: Ptential factors in amyloid plaque formation. *J Neurosci*, 26(40):10129–10140.
19. Du H, et al. (2008) Cyclophilin D deficiency attenuates mitochondrial and neuronal perturbation and ameliorates learning and memory in Alzheimer's disease. *Nat Med*, 14(10):1097–1105.
20. Ren PH, et al. (2009) Cytoplasmic penetration and persistent infection of mammalian cells by polyglutamine aggregates. *Nat Cell Biol*, 11(2):219–225.
21. Gellermann GP, et al. (2006) Alzheimer-like plaque formation by human macrophages is reduced by fibrillation inhibitors and lovastatin. *J Mol Biol*, 360(2):251–257.
22. Hortschansky P, Christopeit T, Schroeckh V, Fandrich M (2005) Thermodynamic analysis of the aggregation propensity of oxidized Alzheimer's beta-amyloid variants. *Protein Sci*, 14(11):2915–2918.
23. Westermark P, et al. Amyloid: Tward terminology clarification report from the Nomenclature Committee of the International Society of Amyloidosis. *Amyloid*, 12(1):1–4.
24. Xue WF, Homans SW, Radford SE (2008) Systematic analysis of nucleation-dependent polymerization reveals new insights into the mechanism of amyloid self-assembly. *Proc Natl Acad Sci USA*, 105(26):8926–8931.
25. Christopeit T, et al. (2005) Mutagenic analysis of the nucleation propensity of oxidized Alzheimer's beta-amyloid peptide. *Protein Sci*, 14(8):2125–2131.
26. Pellarin R, Caflisch A (2006) Interpreting the aggregation kinetics of amyloid peptides. *J Mol Biol*, 360(4):882–892.
27. Meyer-Luehmann M, et al. (2008) Rapid appearance and local toxicity of amyloid-beta plaques in a mouse model of Alzheimer's disease. *Nature*, 451(7179):720–724.
28. Fändrich M, et al. (2003) Myoglobin forms amyloid fibrils by association of unfolded polypeptide segments. *Proc Natl Acad Sci USA*, 100(26):15463–15468.
29. Fändrich M, et al. (2006) Apomyoglobin reveals a random-nucleation mechanism in amyloid protofibril formation. *Acta Histochem*, 108(3):215–219.
30. Jan A, Gokce O, Luthi-Carter R, Lashuel HA (2008) The ratio of monomeric to aggregated forms of Abeta40 and Abeta42 is an important determinant of amyloid-beta aggregation, fibrillogenesis, and toxicity. *J Biol Chem*, 283(42):28176–28189.
31. Saavedra L, Mohamed A, Ma V, Kar S, de Chaves EP (2007) Internalization of beta-amyloid peptide by primary neurons in the absence of apolipoprotein E. *J Biol Chem*, 282(49):35722–35732.
32. Piper RC, Katzmann DJ (2007) Biogenesis and function of multivesicular bodies. *Annu Rev Cell Dev Biol*, 23:519–547.
33. Gouras GK, et al. (2000) Intraneuronal Abeta42 accumulation in human brain. *Am J Pathol*, 156(1):15–20.
34. Billings LM, Oddo S, Green KN, McGaugh JL, LaFerla FM (2005) Intraneuronal Abeta causes the onset of early Alzheimer's disease-related cognitive deficits in transgenic mice. *Neuron*, 45(5):675–688.
35. Crowther DC, et al. (2005) Intraneuronal Abeta, non-amyloid aggregates, and neurodegeneration in a Drosophila model of Alzheimer's disease. *Neuroscience*, 132(1):123–135.
36. Langui D, et al. (2004) Subcellular topography of neuronal Abeta peptide in *APPxPS*1 transgenic mice. *Am J Pathol*, 165(5):1465–1477.
37. Almeida CG, Takahashi RH, Gouras GK (2006) Beta-amyloid accumulation impairs multivesicular body sorting by inhibiting the ubiquitin-proteasome system. *J Neurosci*, 26(16):4277–4288.
38. Nixon RA (2007) Autophagy, amyloidogenesis and Alzheimer disease. *J Cell Sci*, 120(23):4081–4091.
39. Shie FS, LeBoeuf RC, Jin LW (2003) Early intraneuronal Abeta deposition in the hippocampus of APP transgenic mice. *Neuroreport*, 14(1):123–129.
40. Ling D, Song HJ, Garza D, Neufeld TP, Salvaterra PM (2009) Abeta42-induced neurodegeneration via an age-dependent autophagic-lysosomal injury in Drosophila. *PLoS One*, 4(1):e4201.
41. Cataldo AM, Nixon RA (1990) Enzymatically active lysosomal proteases are associated with amyloid deposits in Alzheimer brain. *Proc Natl Acad Sci USA*, 87(10):3861–3865.
42. Roher AE, Palmer KC, Yurewicz EC, Ball MJ, Greenberg BD (1993) Morphological and biochemical analyses of amyloid plaque core proteins purified from Alzheimer disease brain tissue. *J Neurochem*, 61(5):1916–1926.
43. Wilhelmus MM, de Waal RM, Verbeek MM (2007) Heat shock proteins and amateur chaperones in amyloid-Beta accumulation and clearance in Alzheimer's disease. *Mol Neurobiol*, 35(3):203–216.
44. Gomez-Isla T, et al. (1997) Neuronal loss correlates with but exceeds neurofibrillary tangles in Alzheimer's disease. *Ann Neurol*, 41(1):17–24.
45. Duyckaerts C, Potier MC, Delatour B (2007) Alzheimer disease models and human neuropathology: Similarities and differences. *Acta Neuropathol*, 115(1):5–38.
46. Pappolla MA, Omar RA, Vinters HV (1991) Image analysis microspectroscopy shows that neurons participate in the genesis of a subset of early primitive (diffuse) senile plaques. *Am J Pathol*, 139(3):599–607.
47. Nagele RG, Wegiel J, Venkataraman V, Imaki H, Wang KC (2004) Contribution of glial cells to the development of amyloid plaques in Alzheimer's disease. *Neurobiol Aging*, 25(5):663–674.
48. Wisniewski HM, Wegiel J (1994) Beta-amyloid formation by myocytes of leptomeningeal vessels. *Acta Neuropathol*, 87(3):233–241.
49. Wegiel J, Wisniewski HM (1990) The complex of microglial cells and amyloid star in three-dimensional reconstruction. *Acta Neuropathol*, 81(2):116–124.
50. Wisniewski HM, Wegiel J, Wang KC, Lach B (1992) Ultrastructural studies of the cells forming amyloid in the cortical vessel wall in Alzheimer's disease. *Acta Neuropathol*, 84(2):117–127.
51. Röcken C, Shakespeare A (2002) Pathology, diagnosis, and pathogenesis of AA amyloidosis. *Virchows Arch*, 440(2):111–122.
52. Morten IJ, Gosal WS, Radford SE, Hewitt EW (2007) Investigation into the role of macrophages in the formation and degradation of beta2-microglobulin amyloid fibrils. *J Biol Chem*, 282(40):29691–29700.
53. Sommer C, Schröder JM (1989) Amyloid neuropathy: Immunocytochemical localization of intra- and extracellular immunoglobulin light chains. *Acta Neuropathol*, 79(2):190–199.
54. Simard AR, Soulet D, Gowing G, Julien JP, Rivest S (2006) Bone marrow-derived microglia play a critical role in restricting senile plaque formation in Alzheimer's disease. *Neuron*, 49(4):489–502.
55. Gorman PM, Yip CM, Fraser PE, Chakrabartty A (2003) Alternate aggregation pathways of the Alzheimer beta-amyloid peptide: Abeta association kinetics at endosomal pH. *J Mol Biol*, 325(4):743–757.
56. Lomakin A, Teplow DB, Kirschner DA, Benedek GB (1997) Kinetic theory of fibrillogenesis of amyloid beta-protein. *Proc Natl Acad Sci USA*, 94(15):7942–7947.
57. Tashima Y, et al. (2004) The effect of cholesterol and monosialoganglioside (GM1) on the release and aggregation of amyloid beta-peptide from liposomes prepared from brain membrane-like lipids. *J Biol Chem*, 279(17):17587–17595.
58. Möbius W, Herzog V, Sandhoff K, Schwarzmann G (1999) Intracellular distribution of a biotin-labeled ganglioside, GM1, by immunoelectron microscopy after endocytosis in fibroblasts. *J Histochem Cytochem*, 47(8):1005–1014.
59. Iijima K, et al. (2008) Abeta42 mutants with different aggregation profiles induce distinct pathologies in Drosophila. *PLoS ONE*, 3(2):e1703.
60. Yang AJ, Chandswangbhuvana D, Margol L, Glabe CG (1998) Loss of endosomal/lysosomal membrane impermeability is an early event in amyloid Abeta1–42 pathogenesis. *J Neurosci Res*, 52(6):691–698.
61. Habicht G, et al. (2007) Directed selection of a conformational antibody domain that prevents mature amyloid fibril formation by stabilizing Abeta protofibrils. *Proc Natl Acad Sci USA*, 104(49):19232–19237.
62. Ehrnhoefer DE, et al. (2008) EGCG redirects amyloidogenic polypeptides into unstructured, off-pathway oligomers. *Nat Struct Mol Biol*, 15(6):558–566.
63. Klement K, et al. (2007) Effect of different salt ions on the propensity of aggregation and on the structure of Alzheimer's Abeta(1–40) amyloid fibrils. *J Mol Biol*, 373(5):1321–1333.